Journal of The Electrochemical Society, **156** (8) G97-G102 (2009)
0013-4651/2009/156(8)/G97/6/$25.00 © The Electrochemical Society

Using Dielectrophoresis to Trap Nanobead/Stem Cell Compounds in Continuous Flow

Ming-Wen Wang[*,z]

Department of Mechanical Engineering, Oriental Institute of Technology, Pan-Chiao, Taipei Hsien 220, Taiwan

To make the selective sorting of target cells in a multicomponent solution possible, the first step is to use an antigen–antibody reaction to attach antibody-immobilized nanobeads to the surfaces of target stem cells. Later, the resulting nanobead/stem cell compounds are trapped and separated from the mixture by applying other technologies. Creating the compounds makes this subsequent separation possible. To effect the actual separation, a microchannel with multiple electric strips is designed on a silicon substrate and is fabricated with the microelectromechanical systems technology. A local dielectrophoretic force, obtained from nonuniform electric fields, is used to manipulate and trap the compounds in a continuous flow. The experimental studies show that the compounds incur a local dielectrophoretic field when they are suspended in a continuous flow (Re = 5.0) and are exposed to ac fields at a 500 kHz frequency. Using this device, the strip electrodes provide a local dielectrophoretic field strong enough to manipulate and attract nearby compounds in a continuous flow.
 [DOI: 10.1149/1.3138630]

Manuscript submitted December 15, 2008; revised manuscript received April 3, 2009. Published May 28, 2009.

In the form of components such as microchannels, micromixers, and microseparators, microfluidic devices have been widely adopted for many kinds of biological and chemical applications.[1] Most of the chemical and biological reactions are performed in fluid with suspended polymeric beads immobilized by ligands or antibodies. To make the selective sorting of biomolecules in biofluids possible, the first step is to use an antigen–antibody reaction to attach antibody-immobilized nanobeads to the surfaces of the target stem cells.[2,3] Later, the resulting nanobead/stem cell compounds must be trapped and separated from the mixture by applying other technologies.

One of the fundamental difficulties in manipulating the compounds is that most conventional operating tools are orders of magnitude larger than the compounds, which range in size from a few nanometers to micrometers. An additional problem is that a biofluid is an insulator of magnetism and electricity. Several traditional methods utilized to manipulate the compounds have their own limitations and disadvantages. Antibody-based magnetic sorting is among the most useful of such separation technologies because it achieves a rapid and thorough attachment of the antibodies onto the specific target cells.[4] Magnetic separation has also been proven invaluable as a method for the pre-enrichment of complex samples.[5] However, magnetic selection strategies operate with only a single operating parameter (i.e., magnetism), and the development of similar methods capable of enriching multiple distinct species simultaneously has been proven challenging.[6] Of all the microfluidic sorting technologies, the manipulation of biological particles by dielectrophoresis (DEP) is probably the most broadly applied method.[7,8] A dipole movement is induced in the biological particles when they enter an ac field. In an asymmetrical electric field, the polarized particles incur a force that can induce them to move forward to regions of high or low potential field, depending on the polarizability of the particles compared with that of the suspending medium. This force was termed DEP by Pohl.[7,9] Thus by choosing a medium of appropriate conductivity and permittivity, particles of similar dielectric properties can be trapped efficiently. Recent studies have shown that submicron particles can be elegantly manipulated using dielectrophoretic methods. Leukemic cells,[10] breast cancer cells,[11] and CD34 cells[12] can be sorted or enriched from human blood. Combined electrophoretic and dielectrophoretic forces have been used to trap and manipulate DNA on planar microelectrodes.[13-15] However, in the above-mentioned studies, performance was restricted due to the fact that most of the manipulation and separation of submicron particles was performed in a steady pool. Performance in a continuous flow is better and more efficient. Furthermore, only a few experiments have been reported regarding the use of dielectrophoretic manipulation to trap and separate nanobead/stem cell compounds.[11,16-19] Although the multiple dielectrophoresis activated cell sorter has been developed and used to achieve multiple bacterial target cell separation, it is a complex electrode structure that does not allow for a precise manipulation of the hydrodynamic force.[16,20,21] For these reasons, we have conducted a detailed investigation of the mechanisms that enable the trapping of nanobead/stem cell compounds by dielectrophoretic manipulation. The simple arrangement of electrodes that is required is regarded as a promising scheme for future biological studies.

To trap the nanobead/stem cell compounds en masse from the continuous flow mixture, a microfluidic device consisting of a microchannel and multiple electrode strips has been designed and fabricated using the microelectromechanical systems technology. A local dielectrophoretic force obtained from nonuniform electric fields was used to manipulate and trap the nanobead/stem cell compounds in a continuous flow. In this experimental study, the compounds incur positive DEP when suspended in a continuous flow (Re = 5.0). Microelectrodes provide a local dielectrophoretic field strong enough to manipulate and attract nearby compounds in a continuous flow. Experimentation reveals the conditions necessary to enable the trapping of the nanobead/stem cell compounds.

Theoretical Model

Regarding the ac electric charging operation, it can be shown that the time-averaged dielectrophoretic force acting on a cell is given by Pohl[7] and Jones:[8] $F_{DEP} = 2\pi r^3 \varepsilon_m Re\{K(\omega)\} \nabla |E_{rms}|^2$, where r is the radius of the cell, E_{rms} is the root mean square value of the electric field (assuming a sinusoidal time dependence), and $Re\{K(\omega)\}$ depends not only on the dielectric properties of the cell and medium but also on the frequency of the applied field. It is defined as the real part of the Clausius–Mossotti factor, $K(\omega) = (\varepsilon_c^* - \varepsilon_m^*)/(\varepsilon_c^* + \varepsilon_m^*)$. Here the (*) denotes that the dielectric constant is a complex quantity. The complex permittivities of the cell and the medium, ε_c^* and ε_m^*, respectively, are defined as $\varepsilon^* = \varepsilon - j(\sigma/2\pi\omega)$, $j = \sqrt{-1}$, where ε is the permittivity, σ is the conductivity, and ω is the frequency of the applied ac electric field. Variations in this factor give rise to a dielectrophoretic force that is frequency dependent and unique to a particular cell type. For a sphere, the $Re\{K(\omega)\}$ is bounded by the limits $-1/2 < Re\{K(\omega)\} < 1$ and varies with the frequency of the applied field and the complex permittivity of the medium. When positive dielectrophoresis (p-DEP, $\varepsilon_c > \varepsilon_m$) occurs, then $Re\{K(\omega)\} > 0$, the force is directed toward the high potential region of the electric field, and the compounds are attracted toward the edges of asymmetric electrodes. The converse of this is negative dielectrophoresis (n-DEP, $\varepsilon_c < \varepsilon_m$), which leads to $Re\{K(\omega)\} < 0$;

* Electrochemical Society Active Member.
z E-mail: avian@mail.oit.edu.tw

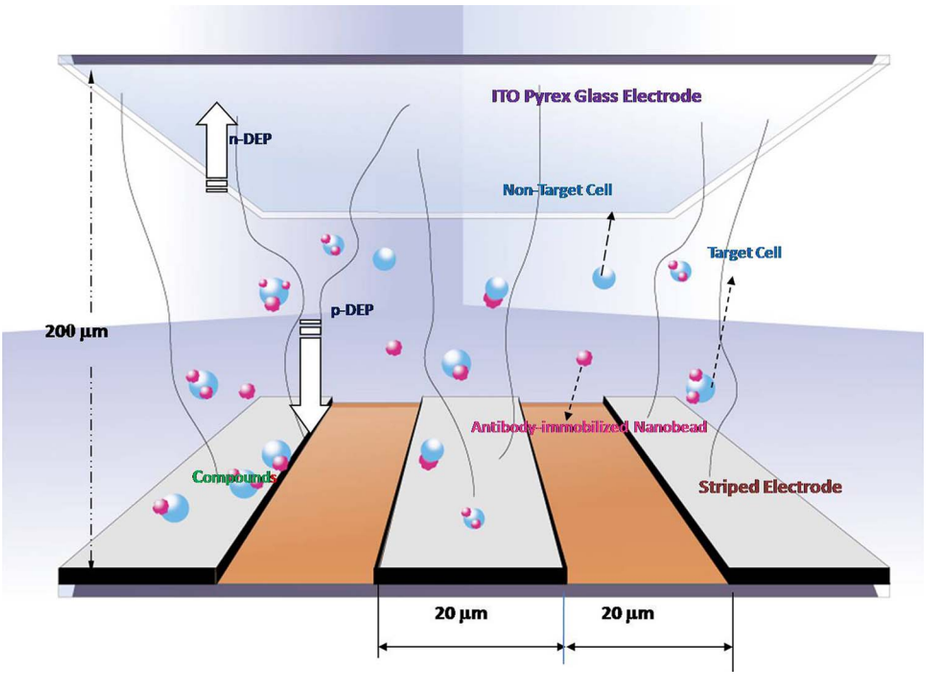

Figure 1. (Color online) Upon experiencing a positive dielectrophoretic force, the nanobead/stem cell compounds are attracted to the high field intensity near the electrode strip. When the nontarget cells are not subjected to a dielectrophoresic force, they pass through the region of the dielectrophoretic field.

in this case, the force is in the direction of decreasing field strength, and the compounds are repelled from the edges of asymmetric electrodes (see Fig. 1).

Ignoring the Brownian motion and buoyancy force, the equation of motion can be written as $m[\mathrm{d}v/\mathrm{d}t] = F_{\mathrm{DEP}} - F_{\mathrm{drag}}$. For low Reynolds numbers, the friction factor for a spherical particle is given by $\zeta = 6\pi r\mu$, where μ is the viscosity of the medium. The instantaneous velocity of cells in a fluid medium is proportional to the instantaneous dielectrophoretic force, so that $U_{\mathrm{DEP}} = F_{\mathrm{DEP}}/\zeta$, or, if we substitute the time-averaged dielectrophoretic force acting on a cell for F_{DEP}, $U_{\mathrm{DEP}} = 2\pi r^3 \varepsilon_{\mathrm{m}} Re\{K(\omega)\} \nabla |E_{\mathrm{rms}}|^2/\zeta$, so that for a spherical particle the dielectrophoretic mobility is given by $U_{\mathrm{DEP}} = r^2 \varepsilon_{\mathrm{m}} Re\{K(\omega)\}/3\mu$ in the direction of $\nabla|E|^2$. Evidently, for a cell the dielectrophoretic mobility depends on the surface area of the particle, together with the real component of the polarizability. Thus dielectrophoretic force could potentially be used to selectively trap the nanobead/stem cell compounds.

Analysis of the electrothermal effect in the fluid medium.— The dielectrophoretic mobility of a particle scales directly with its surface area, so that to manipulate small particles, larger electric-field gradients are required. An applied electric field, coupled with spatial variations in permittivity and conductivity, creates inhomogeneous coulomb and dielectric body forces in a fluid. This phenomenon is known as the electrothermal effect and can induce microscale fluid motion, thereby noninvasively stirring the fluid at the microscale. For a conducting fluid, the power generated is given by $W = \sigma E^2$;[22] the power per unit volume of the electrical field that is absorbed by the fluid is due to Joule heating. Consequently, the temperature of the fluid can be calculated by solving the heat equation with a source term for electrical heat generation: $\rho_{\mathrm{m}} c_{\mathrm{p}}[(\partial T/\partial t) + U_{\mathrm{flow}} \cdot \nabla T] = k\nabla^2 T + \sigma E^2$, where U_{flow} is the velocity of the medium flow, T is the temperature, ρ_{m} is the mass density, c_{p} is the specific heat (at constant pressure), k is the thermal conductivity, and σ is the electrical conductivity of the fluid medium. Temperature dispersion in the continuous flow is affected by advection: the heat equation can be shown as $U_{\mathrm{flow}} \cdot \nabla T = (k\alpha\nabla^2 T/\rho_{\mathrm{m}} c_{\mathrm{p}}) + (\rho E^2/\rho_{\mathrm{m}} c_{\mathrm{p}})$. Following the simplified heat equation, the change in temperature in the medium can be estimated as $\Delta T \sim \sigma V^2/k$ if conduction dominates the heat transfer in the medium. If advection dominates, the change in temperature in the medium can be estimated as $\Delta T \sim \sigma V^2/\rho_{\mathrm{m}} c_{\mathrm{p}} U_{\mathrm{flow}}$. Gradients in temperature produce gradients in permittivity and conductivity in the medium fluid. For the buffer solution, $(1/\sigma)(\partial\sigma/\partial T) = +1\%$ and $(1/\varepsilon)(\partial\varepsilon/\partial T) = +0.5\%$ per kelvin.[23] These variations in electric properties produce gradients in charge density and perturb the electric field.

Experimental

Flow visualization setup.— To analyze the fluidic transport of the beads, a flow visualization system was designed to record the morphogenesis of the antibody-immobilized nanobead/stem cell compounds inside the microfluidic device, as shown in Fig. 2. To illuminate the microfluidic chamber, light from a mercury-arc lamp was directed through a set of epi-optical filters (532 nm). The flow images were captured using a high speed charge-coupled device camera (1000 × 1000 pixels, 12 bit grayscale, and 5000 frames/s, Fastcam SA1, Photron Ltd., Japan) capable of recording 2500 pairs of images via a microscope with an objective lens (M plan Apo Series M = 100, NA = 0.42). The camera offered outstanding light

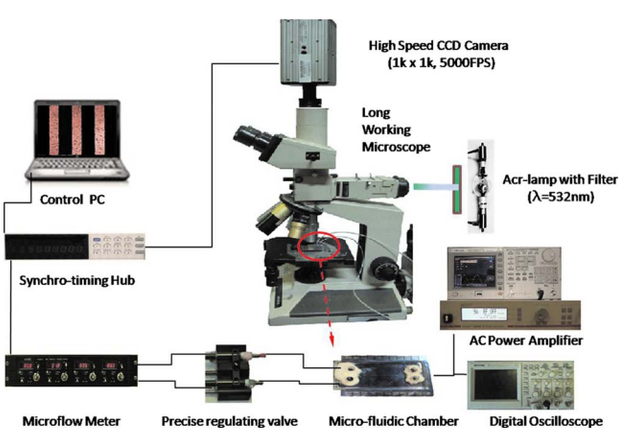

Figure 2. (Color online) Setup of the high speed flow visualization system.

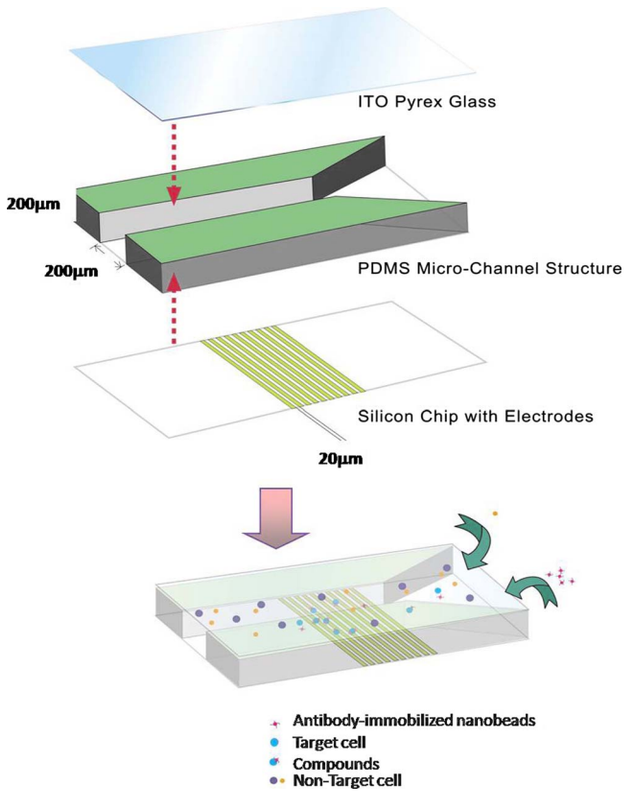

Figure 3. (Color online) The multilayer structure of the microfluidic device with strip electrodes was fabricated by bonding a PDMS replica between an ITO-coated Pyrex glass and a silicon wafer.

sensitivity and brilliant image quality that relied on a 1394 interface connected with a personal computer. Its resolution and decay time were 32l pixel/mm and 2 μs, respectively.

In this study, a filtered illuminant with a wavelength of $\lambda = 532$ nm was used to make the polymeric beads and cells visible in the biological fluid; the diameters of the antibody-immobilized beads and target cells ($d_b \approx 800$ nm, $d_c \approx 3$–5 μm) were larger than the wavelength of the illuminant, i.e., $d_b > \lambda$, and $d_c > \lambda$.

Design of the microfluidic compound trapping device.— A microfluidic trapping device was designed to separate the nanobead/stem cell compounds from the continuous flow mixture. It consists of a microchannel with strip electrodes and was fabricated on a silicon substrate using the microelectromechanical systems fabrication technology. A firm silicone tube connects the microfluidic chamber to a fluid supply system. The biological mixing fluid, composed of the antibody-immobilized nanobeads and stem cells in a buffer solution, is driven by pressurized air and regulated by precision valves. A microflowmeter is used to measure the flow rate. As shown in Fig. 3, the multilayer structure of the microfluidic device, equipped with strip electrodes, was fabricated by bonding a poly(dimethylsiloxane) (PDMS) replica between indium tin oxide (ITO)-coated Pyrex glass (ITO film, 1000 Å) and an electrode-equipped silicon chip. To fabricate the PDMS replica, a microstereolithography system was used to focus radiation onto the surface of a liquid photopolymer resin, forming patterns of a solidified photopolymer. The feature size of the fragment is determined by the diameter of the laser spot focused on the photopolymer surface.[24] Afterward, the master was cleaned with alcohol and deionized water to ease the removal of the PDMS replica from the master after curing. The PDMS prepolymer and a curing agent were mixed in a ratio of 10:1 and then degassed in a vacuum chamber. The polymer mixes were poured onto the master and then cured at 65°C for 1 h.

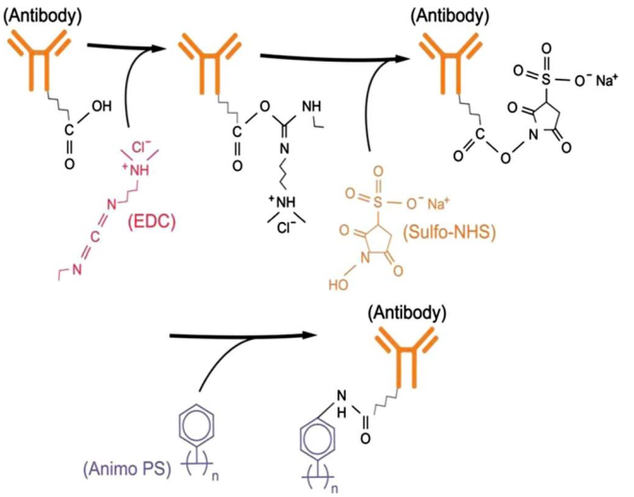

Figure 4. (Color online) Procedure for attaching amine-functionalized polystyrene nanobeads to the antibodies.

After cooling, the PDMS replica was peeled off the master. Asymmetrical microelectrodes, 200 Å Cr and 1000 Å Au, were deposited on the surface of the silicon wafer using a magnetism-enhanced dc sputtering coater, which provided a precise and fast formation of electrodes. Then, to achieve a strong bonding, the PDMS replica was oxidized in a plasma cleaner. Finally the replica was attached to the Pyrex glass slide. The microfluidic device was connected to an ac power amplifier with frequencies in the range of 1 Hz to 10 MHz and voltages of 1–36 V_{pp}. The frequency and magnitude of the applied voltage were probed with a digital oscilloscope (TDS440, Tektronic, LA).

Procedure for attaching amine-functionalized polystyrene nanobeads to the antibodies.— Samples of amine-functionalized nanobeads were prepared from modified polystyrene nanobeads purchased from SPHERO (AP-08-10, diameter $d_b \approx 800$ nm, $\rho = 1.05$ g cm^{-3}, Spherotech, Inc., Lake Forest, IL). A chicken-hosted antihuman bone stem cell CD34 + antibody (XW-7087, CD34 IgY antigen, ProSci Inc., Poway, CA) was purchased from ProSci Co. Amine-functionalized polystyrene nanobeads with surface functional amino groups are very useful for the covalent coupling of the antibody to the surface of the nanobeads using sulfo-NHS (*N*-hydroxysulfosuccinimide sodium salt, $C_4H_4NNaO_6S$, Thermo Fisher Scientific Inc., MA) and EDC (1-ethyl-3-[3-dimethylaminopropyl]-carbodiimide hydrochloride, $C_8H_{17}N_3$–HCl, Sigma-Aldrich Chemie Inc., Steinheim, Germany) in a phosphate buffer (2 mL, 0.1 M, pH 7.4). For 0.2 mL of 5% w/v amine-functionalized polystyrene nanobeads (800 nm), use 2.0 mg of antibody, 20 mg of EDC, and 20 mg of sulfo-NHS. EDC reacts with a carboxyl group on the antibody, forming an amine-reactive *O*-acylisourea intermediate. This intermediate may react with an amine on the amino-functionalized polystyrene nanobead, yielding a conjugate of the two molecules joined by a stable amide bond. However, the intermediate is also susceptible to hydrolysis, making it unstable and short lived in an aqueous solution. The addition of sulfo-NHS stabilizes the amine-reactive intermediate by converting it to an amine-reactive sulfo-NHS ester, thus increasing the efficiency of EDC-mediated coupling reactions. The amine-reactive sulfo-NHS ester intermediate has sufficient stability to permit two-step cross-linking procedures, which allows the carboxyl groups on one antibody to remain unaltered. Figure 4 shows the procedure by which the amine-functionalized nanobeads are joined with the antibodies.

An adult thigh bone marrow solution was provided by the Far Eastern Memorial Hospital. Heparin was added to the sample solu-

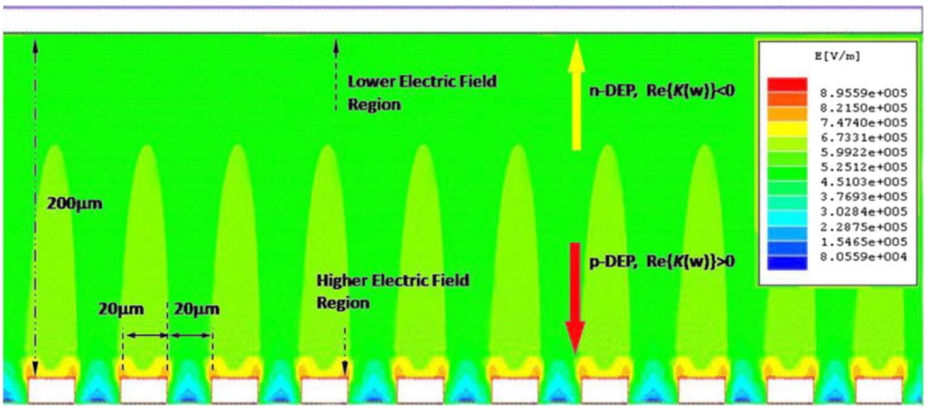

Figure 5. (Color online) Simulation of the electric-field distribution created by strips of microelectrodes.

tion to prevent coagulation. Then the antibody-immobilized nanobeads were dispersed in the bone marrow solution by vigorous stirring, and the antibody-immobilized nanobeads conjoined with the specific stem cells. After the antibody-immobilized nanobeads have attached to the surfaces of the target stem cells, the compounds thus formed can be sorted from the mixing solution using an external electrophoresis force.

Electric-field distribution simulation.— Asymmetrical microelectrodes were used to create the nonuniform field necessary to generate dielectrophoretic forces. The upper electrodes were transparent conducting films, while the lower ones were designed as strips on the surface of the silicon wafer. When the high frequency ac electric charge was applied (20 V_{pp}), the maximum electric field would occur in the region of the lower strip electrodes and the compounds would be trapped. To illustrate this point, a simulation of the electric-field distribution between asymmetrical microelectrodes can be constructed (Fig. 5). To generate a nonuniform electric field across the flow section, the gaps between opposing electrodes were equal to the width of the flow channel. To solve the electromagnetic problem, the electric fields were modeled using ANSOFT Maxwell 3D, a finite element software package. A two-dimensional model was sufficient to describe the electric fields created by the asymmetrical microelectrodes. For simplicity the system was modeled as if it were surrounded by PDMS. The result of the simulation shows that the electric-field distribution is strongest in the vicinity of the strip electrodes. We can make sure that the electric-field gradient is at its maximum in the regions closest to the edge of the strip electrodes; cells which undergo positive DEP should be attracted to those regions.

Results and Discussion

Dielectrophoretic force calculation.— The nanobead/stem cell compounds experience drag force in the buffer solution, given by Stokes law as $F_{drag} = -\zeta v$, where ζ is the friction factor of the compound. A compound moving under the effect of a force F is considered always to move at the terminal velocity F_{DEP}/ζ. For a low Reynolds number, the friction factor for a compound is given as $\zeta = 6\pi\ \mu\ (r_b + r_{cell})$, where μ is the viscosity of the medium. By ignoring Brownian motion and buoyancy, the equation of motion can be written as $m[dv/dt] = F_{DEP} - F_{drag}$. The moving velocity of a compound should be proportional to the time-averaged dielectrophoretic force, so as $U_{DEP} = F_{DEP}/\zeta$, then $U_{DEP} = \{2\pi\varepsilon_m\ \nabla\ |E_{rms}|^2(r_{bead}^3 Re[K(\omega)]_{bead} + r_{cell}^3 Re[K(\omega)]_{cell}\ \}/6\pi\ \mu\ (r_b + r_{cell})\mu$ in the direction of $\nabla|E_{rms}|^2$.

Variations in the Clausius–Mossotti factor give rise to a dielectrophoretic force that is frequency dependent and unique to a particular particle type. For particles the response is dominated by conductivity, which in turn is governed by the surface charge on the particle. The polarizability and the dielectrophoretic force of each particle can be calculated by the dielectrophoretic theory and the total conductivity of particle. However, exposing biological cells to nonuniform electric fields may cause the membrane potential of the cells to rise rapidly.[25,26] Membrane structure conformation and the formation of electropores are changed by increases in the potential of the angled membrane. Electrophoresis increases the conductivity of the membrane, thereby protecting the cell. The creation of electrophoresis was found to start at a membrane potential of 0.5–1 V for several cell types. According to Zimmermann and Neil,[25] an alternating electric field induces a membrane potential on a cell of $V_m = [1.5rE_{rms}\cos\alpha]/[1 + (2\pi\omega\tau)^2]^{1/2}$, where α is the angle between the membrane patch and the field direction, and τ is the relaxation time of the membrane, $\tau = rC_{mem}(\rho_{int} + 0.5\rho_{ext})$, with ρ_{int} and ρ_{ext} denoting the specific resistivity of the interior and the exterior of the cell, respectively, and with C_{mem} representing the specific membrane capacity. The equation is concerned with whether a change in membrane conductivity significantly alters the Clausius–Mossotti factor so that a difference in the total force can be observed at the lower frequencies. This project describes a high frequency operation, ω = 500 kHz, and thus the changes induced in the membrane potential by an alternating electric field will be reduced in an electrical field operating at high frequency. Following the above potential equation, the change in membrane conductivity in the medium can be estimated. Figure 6 shows the frequency dependence of the Clausius–Mossotti factor for the antibody-immobilized nano-

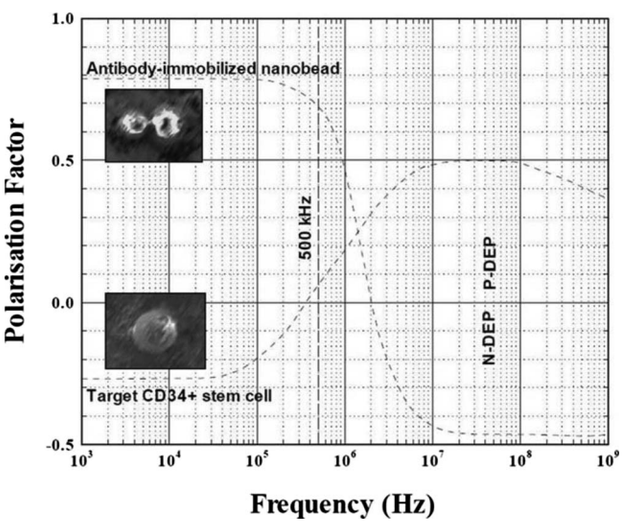

Figure 6. Frequency dependence of the Clausius–Mossotti factor for the antibody-immobilized nanobead ($d_b \approx 800$ nm) and target stem cell ($d_{cell} \approx 3$ μm) with the nanobead permittivity $\varepsilon_b = 2.56$, a medium conductivity $\sigma_m = 1.0$ mS m^{-1}, and the target cell permittivity $\varepsilon_c = 60$.

bead ($d_b \approx 800$ nm) and target stem cell ($d_{cell} \approx 3$ μm) with the nanobead permittivity $\varepsilon_b = 2.56$, a medium conductivity $\sigma_m = 1.0$ mS m^{-1}, and the target cell permittivity $\varepsilon_c = 60$. By the analytic measurement of the zeta potential and the particle size (Brookhaven Zeta PALS, Brookhaven Instruments Co., Holtsville, NY), the total conductance of the target cell σ_c was set at 10 mS m^{-1}, and the antibody-immobilized nanobead σ_b was set at 2.32 nS m^{-1}.

The order analysis is $Re[K(\omega)]_{bead}/Re[K(\omega)]_{cell} \sim O(2)$, $r_{cell}^3/r_{bead}^3 \sim O(3)$, $\{r_{bead}^3 Re[K(\omega)]_{bead} + r_{cell}^3 Re[K(\omega)]_{cell}\} \sim O(1)$, $r_{cell}/r_b \sim O(1)$, and then $\{r_{bead}^3 Re[K(\omega)]_{bead} + r_{cell}^3 Re[K(\omega)]_{cell}\}/6\pi\mu(r_b + r_{cell})\ \mu \sim O(1)$ at the frequency of the applied electric field, $\omega = 500$ kHz. The moving velocity of a compound in the continuous flow is mainly affected by the real part of the Clausius–Mossotti factor of the antibody-immobilized nanobeads, $Re[K(\omega)]_{bead}$. Then, the size effect of the antibody-immobilized nanobeads attached onto the surface of a target cell, $r_{cell}^3 Re[K(\omega)]_{cell}$, would be eliminated by the effect of the friction factor. Consequently, the moving velocity of a compound would be simplified as $U_{DEP} = \{2\pi\varepsilon_m \nabla |E_{rms}|^2 (r_{bead}^3 Re[K(\omega)]_{bead}\}/6\pi\mu r_{bead}$. It can be seen that at a frequency of $\omega = 500$ kHz, the antibody-immobilized nanobeads experience positive DEP, so that the compounds, comprised of the antibody-immobilized nanobeads attached onto the surfaces of the target stem cells, move toward the region of higher field strength.

Additional force effects.— The actual electric field generated in a stasis medium causes high Joule heating, which leads to a rapid temperature rise and induces fluid flow. Local temperature variations in the stasis liquid also bring about permittivity and conductivity inhomogeneities in the medium, which produce a force to activate fluid flow.

Rather than focus in the traditional manner on aspects of cells trapped in a static medium, this project is primarily concerned with the way continuous fluidic flow evokes rapid heat dispersion followed by a continuous flow stream. According to the simplified heat equation, the change in temperature in the fluid, induced by advection in the continuous flow, can be estimated as $\Delta T_{adv} \sim \sigma V^2/\rho_m c_p U$. The number is bigger than that of conduction $\Delta T_{cond} \sim \sigma V^2/k$. For the medium conductivity $\sigma_m = 1.0$ mS m^{-1}, $\rho_m = 1.001 \times 10^3$ kg/m^3, $c_p = 4.182$ kJ/kg K, $V = 20$ V$_{pp}$, $U_{flow} = 4.8 \times 10^{-2}$ m/s, and $k = 0.6$ W/m K, the order analysis is $\Delta T_{cond} \sim O(2)$ and $\Delta T_{adv} \sim O(-1)$, and small gradients in temperature produce smaller gradients in permittivity and conductivity in the medium fluid. According to the results in a static medium,[27] the change in temperature in the fluid approximates 10°C so that the change in temperature in the continuous fluid should be less than 1°C. A general expression of the electrical force per unit volume on an incompressible liquid is $F_{net} = F_{DEP} - F_{electrothermal}$, and $F_{electrothermal} = E_{rms}^2 (1/\varepsilon)(\partial\varepsilon/\partial T)/2$.[22] Because the continuous flow of the fluid does not increase instantaneously in response to the increased temperature, the electrothermal force has a minimal effect on the continuous fluid flow.

Cell–cell interactions constitute an additional force that may affect the trapping of compounds in the buffer nutrient medium. Because the derivation of the DEP force is based on a single compound, cells that disturb the field locally alter the dielectrophoretic force. In this way, forces that attract other compounds and cells may be created. The ratio between the intercell dipole–dipole force and the dielectrophoretic force acting on a single cell can be calculated according to $F_{ratio} \sim [6|K(\omega)|\psi\Delta]/d_{cell}$,[28,29] with ψ as the volume fraction of the cells; Δ is the characteristic length over which the field varies; $d_{cell} \sim r/\psi^{1/3}$, with r being the mean radius of the cells. For the initial density $(4.5–6) \times 10^6$ cell/mL, this ratio is about $2.3–3.5 \times 10^{-7}$, which indicates that the intercell interaction is negligible. When the biological fluid mixes well in the stream flow, there is a corresponding broad decline in cell density, whereby F_{ratio} decreases. The intercell interaction therefore disperses gradually.

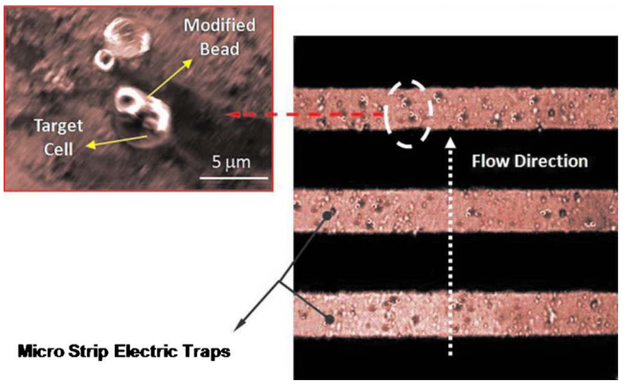

Figure 7. (Color online) Microstrip electric traps provide a local dielectrophoretic field strong enough to attract the compounds (antibody-immobilized nanobeads attached to the surfaces of target stem cells) in the continuous flow.

Dielectrophoretic manipulation.— The observations show the conditions under which it is possible to trap the nanobead/stem cell compounds. At a suitable frequency and applied potential, it was possible to provide a local dielectrophoretic field strong enough to manipulate and attract nearby compounds in a continuous flow ($Re = 5.0$). This can clearly be seen in Fig. 7, which shows the conditions that enabled trapping of the compounds at an applied potential of 20 V$_{pp}$. At a medium conductivity of $\sigma_m = 1.0$ mS m^{-1} and a frequency of 500 kHz, the compounds experience p-DEP, and they move toward the direction of the trap in the main fluid flow, where the dielectrophoretic force is at high strength. In this case, the front strip electrodes supply enough dielectrophoretic force, and the compounds move forward to the rear strip trapping electrodes. The image shows that the compounds are attracted to the high field region of the rear strip trapping electrodes in the downstream direction, and the compounds are widely distributed on the rear strip trapping electrodes. The moving velocity of compounds should be proportioned to the time-averaged dielectrophoretic force, $U_{DEP} = F_{DEP}/\xi$, and then $U_{DEP} = r_{bead}^2 \varepsilon_m Re[K(\omega)]_{bead}\}/3\eta$. Considering the steady-state condition and ignoring the electrothermal effect, the velocity of the compound mobility with ac electric-field application can be expressed as $U_{total} = U_{DEP} + U_{flow}$, and the deviating angle of movement toward the attracting electrodes can be estimated as $\theta \sim \tan^{-1}[\|U_{DEP}\|/\|U_{flow}\|]$, where U_{flow} is the steady flow velocity of continuous flow.

According to the theoretical analysis, $\|U_{DEP}\|/\|U_{flow}\| \sim L_b/L_e$ in a constant time, and the deviating angle can be conveyed to $\theta \sim \tan^{-1}[L_b/L_e]$, where $L_b = 100$ μm is roughly the distance from the main beading flow to the strip trapping electrodes and $L_e = 300$ μm is the range of the dielectrophoresic field provided by the front electrodes, and the deviating angle θ can be expected to fall in the range of 17–20° in the steady state. As measured during the experiment, the approximate value of the deviating angle is 18.5° because the nanobead/stem cell compounds are widely distributed in the region of the rear strip trapping electrodes. The real attaching position deviation of compounds in Fig. 8 has shown that for the real cases of the biological fluid flow considered here, the experiments and theoretical predictions have some similarities. The deviation of the experimental measurements from theoretical predictions may be attributed to the way the discontinuous electrical field in the experimental electrodes differs from the stable electrical field in the

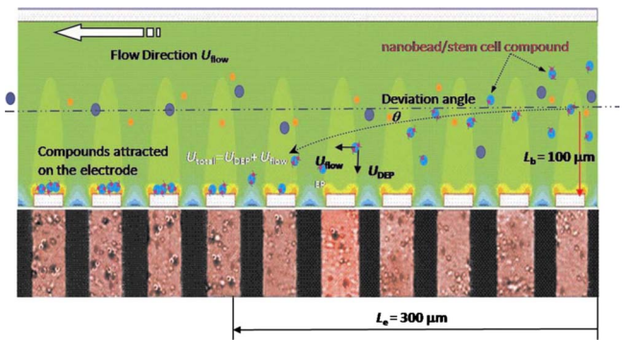

Figure 8. (Color online) Deviation angle of the nanobead/stem cell compounds flowing in the microchannel, $\theta \sim \tan^{-1}[U_b/U_{flow}] \sim \tan^{-1}[L_b/L_e] \sim \tan^{-1}[1/3] \sim 18.5°$, where $L_b = 100$ μm is the distance from the main compounding flow to the attracting electrodes and $L_e = 300$ μm is the range of dielectrophoretic field provided by the strip microelectrodes.

theoretical statement and the fact that the theoretical prediction of the moving velocity of the compound is replaced by actual antibody-immobilized nanobeads.

Conclusions

This work demonstrates that with an appropriate electrode array, a suitable electric field, and the right frequency, compounds formed by attaching antibody-immobilized nanobeads to the surfaces of target stem cells can be trapped and separated out from the fluid mixture. Local dielectrophoretic forces obtained from nonuniform electric fields were used to manipulate and trap the compounds. This technique for the efficient sorting of unique living cells within a biological buffer nutrient medium may potentially allow biological sorting to be performed outside of hospitals, in facilities without a biological analyzing equipment. It has been demonstrated that the deviating mobility of the compounds depends on the polarizability of the antibody-immobilized nanobeads, and this in turn is governed by the dielectric properties of the nanobeads and the medium. Considering the real cases of the nanobead/stem cell compounds, the experimental results and theoretical predictions have some similarities. The slight discrepancy observed between the experimental results and the theoretical predictions is due not only to the qualities of the nonuniform mixture but also to wall roughness. The experiments and theoretical predictions have some similarities. The deviation of the experimental measurements from the theoretical predictions may be attributed to the way the discontinuous electrical field in the experimental electrodes differs from the stable electrical field in the theoretical statement and the fact that the theoretical prediction of the moving velocity of the compound is replaced by actual antibody-immobilized nanobeads. The experimental studies show that the compounds experience p-DEP when suspended in a continuous flow ($Re = 5.0$) and exposed to ac fields at 500 kHz frequency. Using this technique, the strip microelectrodes provide a local dielectrophoretic field strong enough to manipulate and attract nearby compounds in a continuous flow. The observations show the conditions needed to trap the compounds. The results point to the possibility of producing efficient technologies for the continuous flow sorting of biological cells.

Acknowledgments

The author thanks the Far Eastern Memorial Hospital for the preparation of the nanobead/stem cell compounds. Financial support from the Oriental Institute of Technology and National Science Council (grant no. NSC97-2221-E-161-007) of Taiwan is greatly appreciated.

Oriental Institute of Technology assisted in meeting the publication costs of this article.

References

1. N. G. Green, A. Ramos, and H. Morgan, *J. Phys. D: Appl. Phys.*, **33**, 632 (2000).
2. D. B. Weibel, P. Garstecki, D. Ryan, W. R. DiLuzio, M. Mayer, J. E. Seto, and G. M. Whitesides, *Proc. Natl. Acad. Sci. U.S.A.*, **102**, 11963 (2005).
3. H. Zhang, P. S. Williams, W. Zborowski, and J. J. Chalmers, *Biotechnol. Bioeng.*, **95**, 812 (2006).
4. S. Miltenyi, W. Muller, W. Weichel, and A. Radbruch, *Cytometry*, **11**, 231 (1990).
5. L. A. Herzenberg, D. Parks, B. Sahaf, O. Perez, and M. Roederer, *Clin. Chem.*, **48**, 1819 (2002).
6. X. Y. Hu, P. H. Bessette, J. R. Qian, C. D. Meinhart, P. S. Daugherty, and H. T. Soh, *Proc. Natl. Acad. Sci. U.S.A.*, **102**, 15757 (2005).
7. H. A. Pohl, *Dielectrophoresis*, Cambridge University Press, Cambridge, U.K. (1987).
8. T. B. Jones, *Dielectromechanics*, Cambridge University Press, Cambridge, U.K. (1995).
9. H. A. Pohl, *J. Appl. Phys.*, **22**, 869 (1951).
10. F. F. Becker, X. B. Wang, Y. Huang, R. Pethig, J. Vykoukal, and P. R. C. Gascoyne, *J. Phys. D: Appl. Phys.*, **27**, 2659 (1994).
11. F. F. Becker, X. B. Wang, Y. Huang, R. Pethig, J. Vykoukal, and P. R. C. Gascoyne, *Proc. Natl. Acad. Sci. U.S.A.*, **92**, 860 (1995).
12. M. Stephens, M. S. Talary, R. Pethig, A. K. Burnett, and K. I. Mills, *Bone Marrow Transplant*, **18**, 777 (1996).
13. M. Washizu and O. Kurosawa, *IEEE Trans. Ind. Appl.*, **26**, 1165 (1990).
14. M. Washizu, O. Kurosawa, I. Arai, S. Suzuki, and N. Shimamoto, *IEEE Trans. Ind. Appl.*, **31**, 447 (1995).
15. C. L. Asbury and G. van den Engh, *Biophys. J.*, **74**, 1024 (1998).
16. U. Seger, S. Gawad, R. Jogann, A. Bertsch, and P. Renaud, *Lab Chip*, **4**, 148 (2004).
17. U. Kim, J. Qian, S. A. Kenrick, P. S. Daugherty, and H. T. Soh, *Anal. Chem.*, **80**, 8656 (2008).
18. P. H. Bessette, X. Y. Hu, H. T. Soh, and P. S. Daugherty, *Anal. Chem.*, **79**, 2174 (2007).
19. U. Kim, C. W. Shu, K. Y. Dane, P. S. Daugherty, J. Y. J. Wang, and H. T. Soh, *Proc. Natl. Acad. Sci. U.S.A.*, **104**, 20708 (2007).
20. J. G. Kralj, M. T. W. Lis, M. A. Schmidt, and K. F. Jensen, *Anal. Chem.*, **78**, 5019 (2006).
21. P. R. C. Gascoyne and J. Vykoukal, *Electrophoresis*, **23**, 1973 (2002).
22. A. Ramos, H. Morgan, N. G. Green, and A. Castellanos, *J. Phys. D: Appl. Phys.*, **31**, 2338 (1998).
23. *CRC Handbook of Chemistry and Physics*, D. R. Lide, Editor, 88th ed., CRC, London (2008).
24. M. W. Wang and K. H. Teng, *Jpn. J. Appl. Phys., Part 1*, **44**, 2021 (2005).
25. U. Zimmermann and G. A. Neil, *Electromanipulation of Cells*, CRC, Boca Raton, FL (1996).
26. I. Tuval, I. Mezić, F. Bottausci, Y. T. Zhang, N. C. MacDonald, and O. Piro, *Phys. Rev. Lett.*, **95**, 236002 (2005).
27. T. Heida, W. L. Rutten, and E. Marani, *J. Phys. D: Appl. Phys.*, **35**, 1592 (2002).
28. T. B. Jones, *Electromechanics of Particles*, Cambridge University Press, Cambridge, U.K. (1996).
29. A. Dussaud, B. Khusid, and A. Acrivos, *J. Appl. Phys.*, **88**, 5463 (2000).